

# A Life Estimation Method of Peeling in Rolling Bearings Under Mixed Lubrication Conditions

Naoya HASEGAWA \*    Michimasa UCHIDATE \*\*\*  
Takumi FUJITA \*\*    Masayoshi ABO \*\*\*\*

Peeling, which consists of spalls and cracks with the size of about 10  $\mu\text{m}$ , is one of the failures of rolling bearings under boundary and mixed lubrication conditions. In the past, we introduced a life estimation method of peeling which is applicable to boundary lubrication and rolling conditions without slip. In this report, we introduce an updated life estimation method which is applicable to mixed lubrication conditions. The updated method applies a contact analysis based on the load-sharing theory of Johnson et al. This enables us to estimate peeling lives with consideration of the effect of oil film on supporting the load under mixed lubrication conditions. We evaluated the accuracy of the updated method by rolling contact testing. The accuracy of life estimation by the updated method was improved as compared with that of the previous method.

## 1. Introduction

International efforts toward carbon neutrality are expected to further accelerate the use of low viscosity lubricating oil for reducing friction in machinery and automobiles. Low viscosity lubricating oils will increase opportunities for use in boundary lubrication of rolling bearings (hereafter “bearings”) and mixed lubrication conditions (hereafter “severe lubrication conditions”). Improving the reliability of bearings under these conditions is thus expected to be an important technical issue in the future.

Peeling is a typical example of bearing failure that occurs under dilute lubrication conditions. It refers to a dense area of spalling and cracks of about 10  $\mu\text{m}$  in size.<sup>1)</sup> Peeling tends to occur under certain conditions, such as severe lubrication conditions, where the rolling surface oil film parameter  $\lambda$  (the ratio of the minimum film thickness of the rolling area determined by EHL theory to the square root of the root-mean-square roughness of the two surfaces) is low. The cause is thought to be cyclic stress acting on the direct contact area of the surface roughness (hereafter “the real contact area”). In addition, the authors’ research<sup>2,3)</sup> shows that the initial notches of peeling occur because of notch formed by plastic deformation due to the action of the cyclic stress mentioned above.

To examine the reliability of bearings under dilute lubrication conditions, it is necessary to estimate the life as affected by peeling (hereafter the “peeling life”). If the peeling life can be estimated, the surface roughness and lubricant of the bearing can be selected appropriately. In addition, it can also be applied to the design of the surface roughness and lubricating oil viscosity of the bearing necessary to balance reliability

and low torque, which can also help reduce friction for bearing users. In the previous report, the authors introduced a peeling life estimation method<sup>5)</sup> that they independently developed,<sup>4)</sup> but its application was limited to boundary lubrication conditions. In this paper, we present a peeling life estimation method applicable to mixed lubrication conditions, along with the results of validating its estimation accuracy.<sup>5)</sup>

The term “peeling” is customarily used by Japanese domestic bearing manufacturers, while the term “micropitting” is commonly used outside Japan.

## 2. Conventional peeling life estimation method<sup>5)</sup>

### 2.1 Procedure for life estimation

**Fig. 1** shows the procedure for estimating peeling life. In Step 1, rolling fatigue tests are carried out under various operating conditions to obtain a history of peeling life (hereafter “stress history”) and the stress acting on the rolling surface (von Mises stress acting on the depth of 0.5  $\mu\text{m}$  directly below the true contact area, hereafter “surface stress”). Surface stress is reduced during operation by decreasing the surface roughness of the rolling surface and generating compression residual stress (hereafter “running-in”). The surface stress is thus estimated using the results of contact stress analysis and residual stress measurement using the surface roughness measured for each constant load.

The von Mises stress at a depth of 0.5  $\mu\text{m}$  was used for life estimation as the von Mises stress tended to be highest at a depth of 0.5  $\mu\text{m}$  regardless of the test conditions.<sup>5)</sup> In Step 2, the peeling  $S-N$  curve (Stress-Number of cycles to failure) was obtained from the

\* Advanced Technology R&D Center    \*\* Product and Business Strategic Planning Dept.

\*\*\* Faculty of Science and Engineering, Iwate University    \*\*\*\* School of Engineering, University of Hyogo

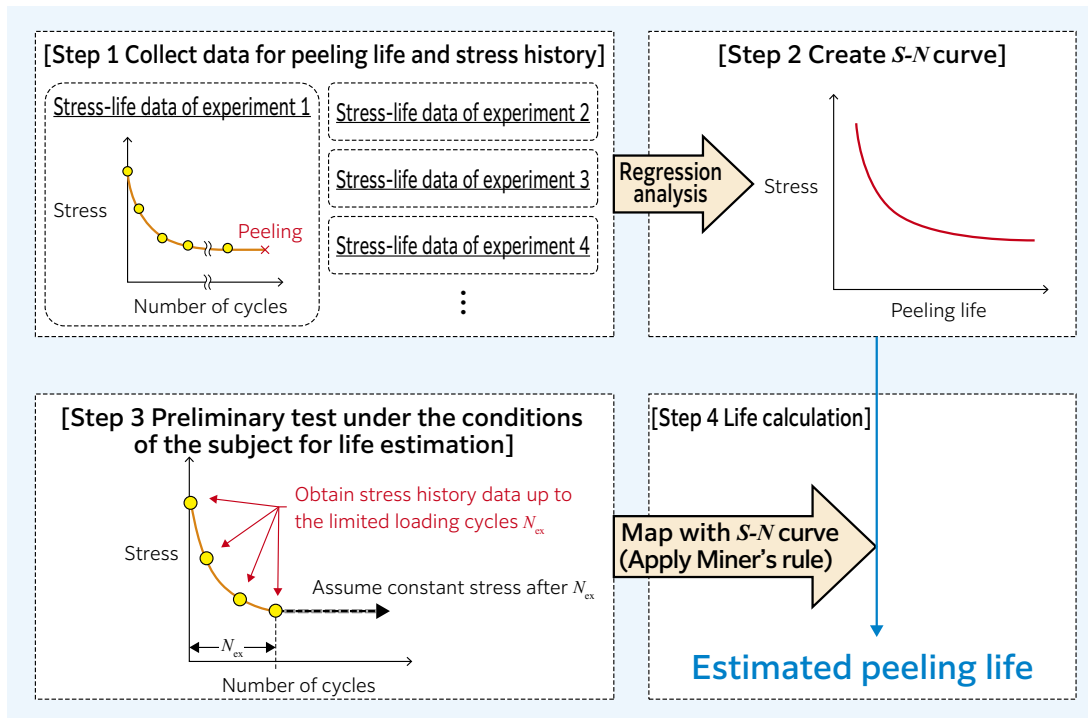


Fig. 1 Flow of the estimation method of peeling life<sup>4)</sup>

peeling life and stress history data obtained in Step 1 by regression analysis. In Step 3, a rolling fatigue test simulating the operating conditions to be estimated (hereafter the “preliminary test”) is conducted to estimate the peeling life under arbitrary conditions, and the stress history under those conditions is obtained. The preliminary test is conducted up to the number of loading cycles when the flexibility stops,  $N_{ex}$  (about  $10^4$  cycles). It is assumed that the surface stress does not change after that time. Finally, in Step 4, the peeling life is estimated using the stress history and  $S-N$  curve obtained in Step 3.

In Steps 2 and 4 of this procedure, the degree of fatigue (the ratio of the total number of loads to the lifetime) is calculated using Miner’s law from the stress history. The concept adopted is that peeling occurs when the degree of fatigue reaches 100 %.

For surface stress, the average value of von Mises stress acting at a depth of  $0.5 \mu\text{m}$  below the individual real contact area is used. To obtain this, the normal stress component  $\hat{\sigma}_j$  and the shear stress component  $\hat{\tau}_{jk}$  of the triaxial stress acting substantially at a depth of  $0.5 \mu\text{m}$  below the true contact area are first determined by the following equations (1) and (2).

$$\hat{\sigma}_j = \sigma_{j, \text{con}} + \sigma_{j, \text{res}} \quad (1)$$

$$\hat{\tau}_{jk} = \tau_{jk, \text{con}} + \tau_{jk, \text{res}} \quad (2)$$

$$(j = x, y, z, k = x, y, z, j \neq k, \tau_{jk} = \tau_{kj})$$

Here, the subscript “con” indicates the contact stress obtained by contact stress analysis, and “res” indicates the residual stress obtained by residual stress measurement. In addition, x represents the circumferential direction, y the axial direction, and z the depth direction in the rolling surface. The triaxial stress components obtained in equations (1) and (2)

are then substituted into equation (3) below to obtain the von Mises stress at a depth of  $0.5 \mu\text{m}$  at the real contact area, and the surface stress is obtained as the average of these values.

$$\sigma_{vm} = \sqrt{\frac{1}{2} \{ (\sigma_x - \sigma_y)^2 + (\sigma_y - \sigma_z)^2 + (\sigma_z - \sigma_x)^2 + 6 (\tau_{xy}^2 + \tau_{yz}^2 + \tau_{zx}^2) \}} \quad (3)$$

Although this estimation method requires preliminary testing, the life can be estimated in a few hours, including preliminary testing. By using the data from the preliminary tests, it is possible to perform a life estimation that accurately reflects running-in behavior under a wide variety of conditions that are difficult to simulate. Another feature of this method is that it takes into account the effect of residual stress on the life. The  $S-N$  curves should be prepared for each steel grade and heat treatment of rolling parts.

### 3. Improved method of contact stress analysis for application to mixed lubrication conditions

#### 3.1 Overview of contact stress analysis

Under mixed lubrication conditions, the effect of load support by the oil film cannot be ignored. In this paper, to apply the peeling life estimation method described above to mixed lubrication conditions, the contact stress analysis for estimating surface stress was enhanced to a method<sup>7)</sup> that can consider the effect of load support by the oil film. In this analysis, the load sharing theory<sup>8)</sup> of Johnson et al. is applied. The load on the rolling parts is considered to be shared by the oil film and the true contact area at a certain ratio, as shown in Fig. 2. The pressure distribution on the rolling surface is therefore obtained as the sum of

the pressure distributions of the oil film and the true contact area. The pressure distributions of the oil film and the true contact area are determined separately by convergence calculations with the load sharing ratio of the oil film as an unknown quantity. The convergence condition here is that the mass of the oil film in the clearance between two rough surfaces is equal to the mass of oil film formed between two smooth surfaces when the sharing load of oil is applied.

Hereafter, the procedure of this analysis is described with reference to **Fig. 3**. In Step 1, the load sharing ratio of the oil film to the load  $W$  on the rolling area is set as  $\alpha$ . Then, the central oil film thickness  $h_c$ , the distribution of oil film pressure  $P_f(x, y)$ , and the elastic deformation of the two surfaces are calculated under the condition in which the sharing load of oil  $\alpha W$  is applied to smooth surfaces. An arbitrary initial value is set for  $\alpha$  in this calculation. The central oil film thickness  $h_c$  is calculated with the formula<sup>9)</sup> of central oil film thickness of Chittenden et al, and the correction coefficient<sup>10)</sup> due to shear heating. The oil film pressure  $P_f(x, y)$  and the elastic deformation are assumed to be equal to them when the two surfaces contact with the load  $\alpha W$ , and are obtained by the contact calculation program<sup>11)</sup> using the boundary element method. This is based on the fact that the spike of oil film pressure under high pressure conditions (several GPa) is small and negligible.<sup>12)</sup> Besides, the lubrication regime of rolling bearings is generally the E-V (Elastic-Variable viscosity) regime in which the viscosity of the oil increases with the rise in pressure and the deformation of the rolling surface due to hydraulic pressure cannot be ignored. However, under conditions where  $\alpha$  is close to 0, the lubrication regime is not E-V regime. In that case, the Chittenden et al. formula cannot be applied. Nevertheless, the error of analysis due to applying the formula of Chittenden et al. may be small as the influence of the oil film on the load support is small when  $\alpha$  is close to 0. In Step 2, the three-dimensional roughness data of the rolling surface actually measured in advance is added to the shape of the two surfaces after the elastic deformation obtained in Step 1, and the rough surface shape of the deformed state due to the action of hydraulic pressure (hereafter, the rough surface

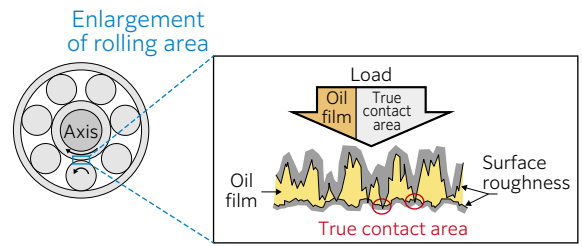


**Fig. 2** Concept of load sharing theory

shape after hydraulic action) is created.

In Step 3, the remaining load  $(1 - \alpha)W$  is applied to the rough surface shape after the hydraulic action, and the distribution of pressure  $P_a(x, y)$  at the true contact area and the average clearance  $h_{m, rough}$  of the two surfaces are calculated using the same contact calculation program as in Step 1. The average clearance  $h_{m, rough}$  is calculated by the following equations.

$$h_{m, rough} = \int_A h_{rough}(x, y) dx dy / A \quad (4)$$

In the formula (4),  $A$  is the area of the region where the oil film pressure  $P_f(x, y)$  is greater than 0 in Step 1. In addition, the clearance at the true contact area is set to 0. In Step 4, we examine whether the central oil film thickness  $h_c$  found in Step 1 is equal to the average clearance  $h_{m, rough}$  found in Step 3. If it is not equal, we return to Step 1 and correct  $\alpha$ . This is the convergence condition of the contact stress analysis, and is based on the idea that the mass of the lubricating oil drawn in between the two surfaces does not change regardless of the surface roughness of the two surfaces (law of conservation of mass). In Step 5, the pressure distribution  $P(x, y)$  on the rolling surface when the total load  $W$  is applied is determined as the sum of  $P_f(x, y)$  and  $P_a(x, y)$ , then the elasticity solution of Boussinesq<sup>13)</sup> is applied to the obtained pressure distribution. In this way, the distribution of internal stresses (triaxial stress components) below the rolling surface is calculated.

### 3.2 Validity of contact stress analysis

The value of the load sharing ratio  $\alpha$  and surface stress of the oil film obtained by this analysis method was verified to match the index of oil film formability obtained in the rolling fatigue test and the residual stress

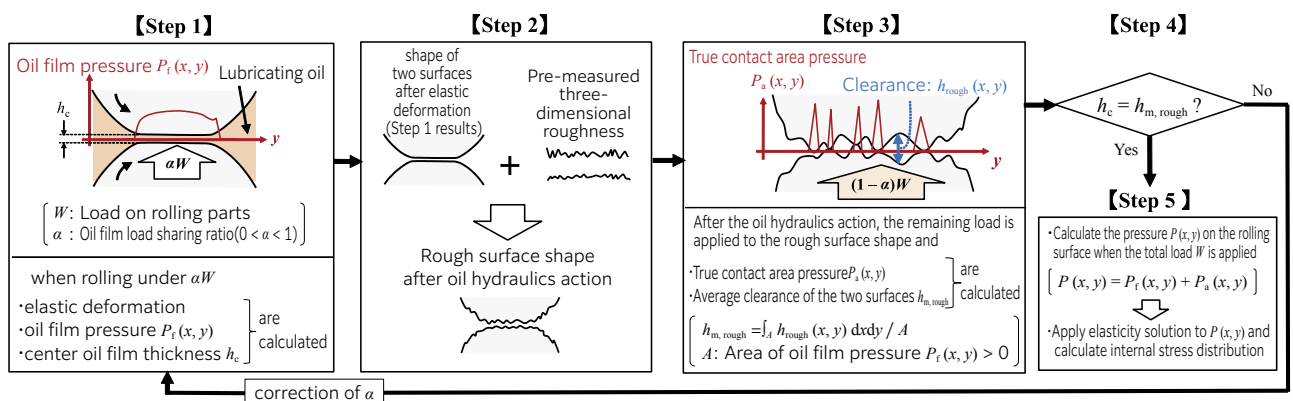


**Fig. 3** Contact Stress Analysis Procedure<sup>7)</sup>

change of the test piece.<sup>7)</sup> Although details are omitted in this paper, it has been confirmed that the analytical values of  $\alpha$  and surface stress are generally consistent with the test data. **Fig. 4** shows, as an example of the results of the study, the relationship between the estimated value of the surface stress of the rolling surface and the measured value of the residual stress in the rolling fatigue test.

The rolling fatigue tests were conducted in a two-roller testing machine, as described below, with a gradually decreasing rotational speed starting at 900 min<sup>-1</sup>. The test was interrupted each time when the rotational speed was changed, and the three-dimensional roughness and residual stress of the rolling surface were measured at each interruption. From these measurements, the surface stress during the test at each rotational speed was estimated. **Fig. 4** shows that the surface stress (estimated value) during operation exceeded the yield stress of the test piece at a rotational speed of 125 min<sup>-1</sup>. The residual stress (measured value) increased during operation at a rotational speed of 125 min<sup>-1</sup>. These results are consistent with the prediction of the contact analysis that the rolling surface shows plastic deformation at 125 min<sup>-1</sup> and the validation of the residual stress measurements.

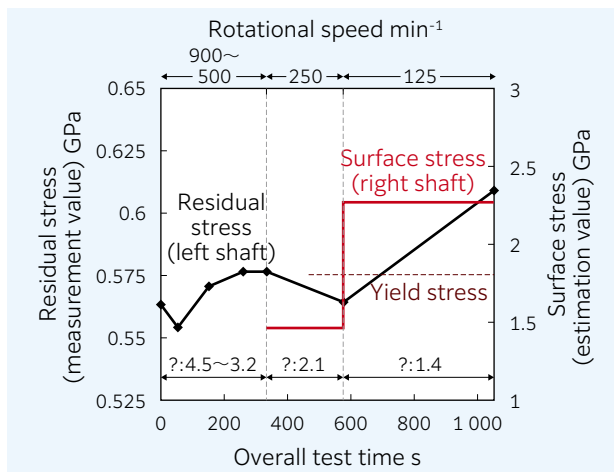


**Fig. 4** Relationship between surface stress estimated by contact stress analysis and measured residual stress<sup>7)</sup>

4. Life estimation overall accuracy verification

4.1 Rolling fatigue test

To verify the accuracy of the new life estimation method, rolling fatigue tests were carried out with the two-roller testing machine shown in **Fig. 5**. The drive roller and the driven roller were cylindrical with an outer diameter of  $\phi$  40 mm and a thickness of 12 mm. A radius of 60 mm was applied to the drive roller only in the axial direction. A felt pad impregnated with lubricating oil was used to lubricate the roller test piece by contacting it from below. The material of the roller test piece was SUJ2, which was subjected to standard quench-hardening and tempering so that the surface hardness was about 63 HRC. **Table 1** shows the test conditions. Testing was carried out under varying conditions in terms of the surface roughness of the rolling surface, the rotation speed, the maximum hertzian contact surface pressure, and the lubricating oil type. The  $\lambda$  of Nos. 6 and 7 tests is more than 0.5, which corresponds to the mixed lubrication condition. Since it is easy for peeling to occur in the driven roller, which has low surface roughness, the life was determined from the occurrence of the peeling on the driven roller. In principle, each test was interrupted at 10<sup>2</sup> cycles, 10<sup>3</sup> cycles, 5 × 10<sup>3</sup> cycles, 10<sup>4</sup> cycles, and 10<sup>5</sup> cycles at load. At these interruptions and before the test, the three-dimensional roughness measurement of the drive roller and the driven roller and the residual stress measurement of the driven roller were performed. The stress history of the driven roller was obtained from the collected data. In addition, the occurrence status of the peeling of the driven roller was observed with an optical microscope at the time of interruption. The total number of loads when the ratio of the area of the occurrence of micro spalling and cracks to the area of the observation field of view (hereinafter referred to as the peeling area ratio) reached 0.5 % or more at six different places in the rolling surface was taken as the actual life  $L_{act}$  of the peeling. If the peeling area ratio was less than 0.5 % at 10<sup>5</sup> cycles, the test was continued until 0.5 % was reached.

**Table 1** Test conditions of the two-roller test<sup>6)</sup>

Test No.	Surface roughness ( $R_a$ ) $\mu$ m		Rotational speed min <sup>-1</sup>	Maximum Hertzian contact pressure GPa	Lubricant	Dynamic viscosity (40 °C) mm <sup>2</sup> /s	Oil film parameter $\lambda$	
	Drive roller	Driven roller						
1	0.75	0.02	2 000	2.3	Synthetic oil (PAO)	6.2	0.11	
2							0.12	
3							0.06	
4							0.17	
5	0.50		0.52					
6	0.75		32.6	0.87				
7	0.40		500	2.3	Mineral oil	47.7	0.15	
8							6.8	0.17
9								
10					0.24			
11	0.35		2 000	2.3	Synthetic oil (PAO)	6.2	0.24	

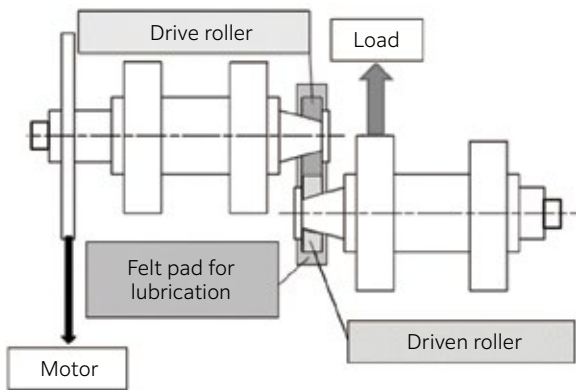


**Fig. 5** Two-roller testing machine<sup>2)</sup>

#### 4.2 Method for verification of overall estimation accuracy

Peeling life was estimated for the two-roller testing machines Nos. 1 to 11 shown in **Table 1** by the procedure shown in **Fig. 1**. The life was estimated with and without considering the load sharing theory in the contact stress analysis, and the accuracy of the life estimation was compared between the two cases. The estimated peeling life  $L_{est}$  for each test was calculated from the stress history up to  $10^4$  cycles. For the life estimation with load sharing theory,  $S-N$  curves were generated using the test data except for Nos. 7 and 8, which were used for the calculation of  $L_{est}$ . In the case of life estimations where the load sharing theory was not considered,  $L_{est}$  was calculated using the  $S-N$  curve that had already been created in a previous report.<sup>5)</sup> The overall accuracy of the life estimation was examined using the life ratio ( $L_{act} / L_{est}$ ) between  $L_{est}$  and the actual life of the peeling,  $L_{act}$ , which was finally obtained in the test.

### 5. Results

**Fig. 6** shows the relationship between the estimated life  $L_{est}$  and the actual life  $L_{act}$ . The median, minimum, and maximum values of the life ratio ( $L_{act} / L_{est}$ ) are

also shown in the figure. In the case of **Fig. 6** (a) without consideration of load sharing theory, the overall accuracy of life estimation for tests Nos. 6 and 7, which were conducted under mixed lubrication conditions, was lower than that of the other tests, and the error in estimated life relative to actual life (the error is calculated as the largest value or the reciprocal of the minimum value of  $L_{act} / L_{est}$ ) was 20 times. On the other hand, when the load-sharing theory is taken into account in **Fig. 6** (b), the error in the estimated overall accuracy for tests Nos. 6 and 7 is less than five times, indicating that the overall accuracy of life estimation under mixed lubrication conditions is improved. Considering that the life of bearings generally varies by a factor of 10 or more under the same conditions<sup>14)</sup>, the overall accuracy of the life estimation in the case of the load sharing theory is considered to be at a sufficiently high level for practical use.

### 6. Summary

This article has presented an improved peeling life estimation method applicable to mixed lubrication conditions and the results of validation of the overall accuracy of the life estimation.

- 1) In this estimation method, a method of contact stress analysis that applies load sharing theory is employed, and the effect of lubrication conditions on peeling life is considered.
- 2) The maximum error of the peeling life obtained by this estimation method is less than 5 times of the actual life, and the accuracy of the peeling life estimation under mixed lubrication conditions is improved compared to the conventional method. The overall accuracy of the above is sufficiently high for practical use as a peeling life estimation method for bearings.

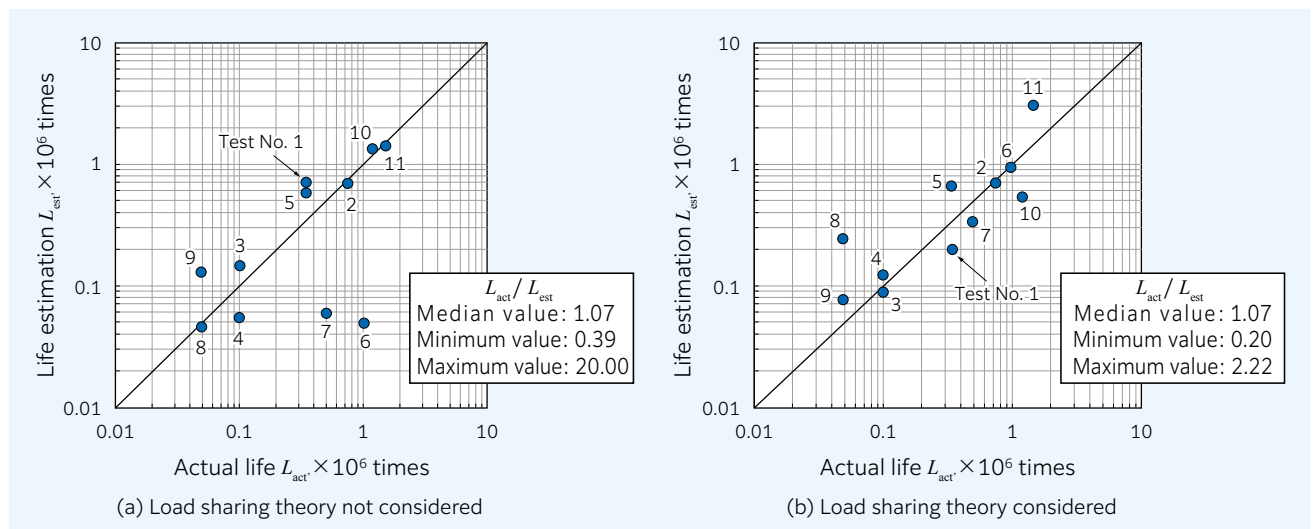


**Fig. 6** Relationship between estimated peeling lives and actual peeling lives<sup>6)</sup>

It should be noted that the scope of application of this estimation method is currently limited to pure rolling conditions. Going forward, we will work to further improve the accuracy of the estimation and extend it to conditions where there is slip on the rolling surface. This estimation technique will be used to provide customer value in the form of improved bearing reliability and higher machine efficiency.

This paper summarizes the content of the presentation “Estimation Method of Micropitting Life from  $S-N$  Curve Established by Residual Stress Measurements and Numerical Contact Analysis, 2nd Report” in the Proceedings of Tribology Congress 2021 Spring Tokyo, which was organized by the Japanese Society of Tribologists and the presentation “Validation of Contact Stress Analysis of Rolling Surface under Mixed Lubrication” in the Proceedings of Tribology Congress 2022 Spring Tokyo. (Some figures and tables have been translated into Japanese and rearranged.) We thank the Japanese Society of Tribologists for their kind permission to publish this paper.

### References

- 1) Noriyuki Tsushima, Hirokazu Nakashima, Hiroshi Kashimura: Typical Failures of Bearings, NTN TECHNICAL REVIEW, No. 57 (1990) 59.
- 2) Naoya Hasegawa, Takumi Fujita, Michimasa Uchidate, Masayoshi Abo: Mechanism for Initiation of Peeling in Rolling Contact and the Effect of Black Oxide Treatment on the Suppression of Peeling (Part 1), The Tribologist, 63, 8, (2018) 551.
- 3) Naoya Hasegawa, Takumi Fujita, Michimasa Uchidate, Masayoshi Abo, Mechanism for Initiation of Peeling in Rolling Contact and the Effect of Black Oxide Treatment on the Suppression of Peeling (Part 2), The Tribologist, 63, 9, (2018) 618.
- 4) N. Hasegawa, T. Fujita, M. Uchidate, M. Abo, and H. Kinoshita: Initiation Mechanism of Peeling in Rolling Bearings, and Its Life Estimation Method, NTN TECHNICAL REVIEW, No. 88, (2021) 77.
- 5) N. Hasegawa, T. Fujita, M. Uchidate, M. Abo & H. Kinoshita, Estimation Method of Micropitting Life from  $S-N$  Curve Established by Residual Stress Measurements and Numerical Contact Analysis, Tribology Online, 14, 3, (2019) 131.
- 6) N. Hasegawa, T. Fujita, M. Uchidate, and M. Abo: Estimation Method of Micropitting Life from  $S-N$  Curve Established by Residual Stress Measurements and Numerical Contact Analysis, 2nd Report, Proceedings of Tribology Congress 2021 Spring Tokyo, (2021) B22.
- 7) N. Hasegawa, T. Fujita, and M. Uchidate: Validation of Contact Stress Analysis of Rolling Surface under Mixed Lubrication, Proceedings of Tribology Congress 2022 Spring Tokyo, (2022) F11
- 8) K. L. Johnson, J. A. Greenwood & S. Y. Poon, A Simple Theory of Asperity Contact in Elastohydrodynamic Lubrication, Wear, 19, (1972) 91-108.
- 9) R. J. Chittenden, D. Dowson, J. F. Dunn & C. M. Taylor, A Theoretical Analysis of the Isothermal Elastohydrodynamic Lubrication of Concentrated Contacts, II. General Case, With Lubricant Entrainment Along Either Principal Axis of the Hertzian Contact Ellipse or at some Intermediate Angle, Proc. Roy. Soc. Lond., A, 397, (1985) 271-294.
- 10) M. K. Ghosh and R. K. Pandey, Thermal Elastohydrodynamic Lubrication of Heavily Loaded Line Contacts-An Efficient Inlet Zone Analysis, Trans. ASME, J. Tribol., 120-1, (1998) 119-125.
- 11) M. Uchidate, Comparison of Contact Conditions Obtained by Direct Simulation with Statistical Analysis for Normally Distributed Isotropic Surfaces, Surface Topography: Metrology and Properties, 6, 3, (2018) 034003.
- 12) H. Takada and R. Aihara, Life and Reliability of Rolling Bearings, Nikkan Kogyo Shimbun, (2005) 161.
- 13) K. L. Johnson, Contact Mechanics, Cambridge University Press, Cambridge, (1985) 51.
- 14) Rolling Bearing Operating Life Study Group, Influence of Load and Lubricant on the Life of Rolling Bearing, The Tribologist, 61, 9, (2016) 607

Photo of authors



Naoya HASEGAWA

Advanced  
Technology R&D  
Center



Takumi FUJITA

Product and  
Business Strategic  
Planning Dept.



Michimasa UCHIDATE

Faculty of Science  
and Engineering,  
Iwate University



Masayoshi ABO

School of  
Engineering,  
University of Hyogo